Supplementary Materials for

Mitochondrial introgression shows extensive hybridization events among *Saccharomyces* species

Authors: David Peris, Armando Arias, Sandi Orlić, Carmela Belloch, Laura Pérez-Través, Amparo Querol, Eladio Barrio

Correspondence to: david.perisnavarro@wisc.edu

This PDF file includes:

Supplementary Text

Table of Contents

Supplementary Text

COX2 nucleotide statistics

A total of five hundred and seventeen *COX2* sequences of worldwide distributed wild *Saccharomyces* strains and forty-nine sequences of domesticated natural hybrids were sequenced or retrieved from public databases (Table S1, Figure 1). The *COX2* alignment is 585 bp, with 106 variable positions (18.11%) (Figure S2) where 43.4% of polymorphisms are found in the last 89 nucleotides. 80 of the variable positions are phylogenetically informative. 27 variable sites correspond to 0-fold degenerated, but only 10 of them are informative. 20 variable sites correspond to 2-fold degenerated positions (19 informative and 1 singleton), being 5 of them non-synonymous substitutions. Finally, 42 variable sites are 4-fold degenerated and 38 of them are informative.

COX2 genetic diversity statistics are summarized in Table S3. The most diverse sequences were found in three species, *S. cerevisiae, S. paradoxus* and *S. mikatae*. In the case of *S. cerevisiae* nucleotide diversity values of 2.1% are so much higher than values inferred for the nuclear genome, around 0.9% (Liti *et al.* 2009), suggesting that recombination is increasing the values. For *S. eubayanus* and *S. uvarum*, the *COX2* nucleotide diversity values, 0.5 and 0.6% respectively, are lower than those found for the nuclear genome, around 0.8% (Patagonia A-Patagonia B *S. eubayanus*) and 1% (Holarctic-South America B *S. uvarum*) (Almeida *et al.* 2014; Peris *et al.* 2014) in agreement with the low mutation rate of yeast mitochondrial genomes (Clark-Walker 1991). *COX2* values for *S. kudriavzevii* strains are similar to those inferred for the nuclear genome, 1.11% (Hittinger *et al.* 2010).

Maximum-Likelihood phylogenetic tree of *COX2* 3'end region is incongruent with the species tree due to a recombination hotspot

COX2 alignment was split in two segments based on the most common recombination point. We reconstructed the Maximum-Likelihood tree with `PhyML v3.0` (Guindon and Gascuel 2003) using the best fitted substitution model inferred by `jModeltest` (Posada 2008). Phylogenetic trees comparison with the *Saccharomyces* species tree was performed in `Tree Puzzle v5.2` (Schmidt *et al.* 2002) implemented with the conservative Shimodaira-Hasegawa (Shimodaira and Hasegawa 1999) and Expected

Likelihood weights (ELW) (Strimmer and Rambaut 2002) tests. Both *COX2* 5'end segment and the species tree agree each other; however, the *COX2* 3'end was best explained by the inferred ML using that sequence region, and significantly rejected the topology of the species tree (p-value < $1*10^{-5}$), suggesting incongruence between the inferred ML *COX2* 3'end phylogenetic tree and the species tree.

A set of *COX2* representative sequences of each haplotype was the input of `RDPv3.44` package (Martin *et al.* 2010). RDP includes six methods to detect recombination: RDP (Martin and Rybicki 2000), Bootscanning (Salminen *et al.* 1995), MaxChi (Smith 1992), Chimaera (Smith 1992), GeneConv (Padidam *et al.* 1999) and Sis-scan (Gibbs *et al.* 2000). Default settings were set up with a statistical significance threshold of p-value < 0.05, with Bonferroni correction for multiple comparisons.

Codons (nucleotide sequences 526-528 and 535-537) in the *COX2* 3' end show several convergent nucleotide substitutions among *S. cerevisiae* and *S. paradoxus* strains. This finding might be the result of a "patchy-tachy" effect due to different substitution rate in those positions (Sun *et al.* 2011). Homoplasies can drive to recombinant false positives. One confounding effect can be observed in L1528 and CECT11757 strains which is difficult to know if they were truly introgressed or they suffered two different recombination events with two different *S. paradoxus* lineages, Far Eastern and European. A recent study shown transfers from European *S. paradoxus* GC42 cluster to *S. cerevisiae* L1528 (Wu and Hao 2015). Also the presence of type II *ORF1* segments supports the introgression scenario and a double recombination scenario.

***ORF1* gene structure**

52 different haplotypes were found in our representative strains (Table S1). *ORF1* start codon is nineteen nucleotides inside the 3' end of COX2 gene. The average GC-composition of the ORF1 is extremely low, 18%. Eleven strains have a GTG as a start codon, which is uncommon in yeast mitochondria: haplotypes M2-M7 and M9-M12. The translation of the *ORF1* gene predicts fourteen strains having a premature stop codon: haplotypes M2, M3, M7-M11, M17-M20, M23 and M46. *ORF1* sequence length range from 1363bp (*S. cerevisiae* ZA17 strain) to 1516bp (*S. cerevisiae* VRB strain), translated

to 454 and 505, respectively. Note that we sequenced a partial *ORF1* gene, and the last 45 nucleotides were not sequenced in this study.

ORF1 secondary structure and domains (LAGLIDADG and NUMOD) were annotated in Jalview according to Dalgaard *et al.* (Dalgaard *et al.* 1997) and using the Conserved Domains tool in NCBI (http://www.ncbi.nlm.nih.gov/Structure/cdd/ wrpsb.cgi) (Marchler-Bauer *et al.* 2009). WebLogo profiles of LAGLIDADG and NUMOD1 domains were done in WebLogo 2.8.2 tool (http://weblogo.berkeley.edu/). Three different domains were found in all *ORF1* sequences: two LADGLIDADG (P1 and P2) and one NUMOD1 (Figure 6, S9 and S10). Two non-*Saccharomyces ORF1* were detected by PSI-BLAST (Altschul *et al.* 1997) showing some similarities with the *Saccharomyces ORF1* sequences. We generated a new alignment in Jalview 4.0.b2 (Waterhouse *et al.* 2009) including the *Cyberlindnera* (*Williopsis*) *saturnus* var. *suaveolans* (*ORF1* and *ORF3*), and one from *Kazachstania servazii* (SasefMp08) sequences (Figure S10). The sequence from *K. servazii* was found to be closely related to the *Saccharomyces ORF1* sequences (Figure S3). Although, *C. saturnus* is phylogenetically fairly distant from *Saccharomyces* genus (James SA *et al.* 1998), they have been diverging since 235mya, we observed some conservation among LAGLIDADG and NUMOD aminoacids when compared with *Saccharomyces* and non-*Saccharomyces ORF1* sequences (Figure S9 and S10).

Differences in size among *ORF1* gene sequences were due to the presence of GC insertions (Figure S3) and AT repeats (Table S4). Seven different GC clusters insertion points were found along the *ORF1* alignment. GC cluster 1 is observed in *S. cerevisiae* VRB; three types of GC cluster 2 were found in *S. cerevisiae* CBS435, CECT11757, and *S. paradoxus* 120MX (Figure S3 and S11); GC cluster 3 is shown in *S. arboricola* CBS10644; GC cluster 4 is shown in *S. cerevisiae* VRB; GC cluster 5 is inserted in *ORF1* of *S. cerevisiae* CBS435, and was structurally similar to GC cluster 3 of *S. arboricola* CBS10644; GC cluster 6 and 7 were the most frequent among *Saccharomyces* strains (Figure S3 and S12). 40 *S. cerevisiae* and one hybrid *S. cerevisiae* x *S. kudriavzevii* (AMH) have the GC cluster 6, and 36 *S. cerevisiae*, 2 hybrids *S. cerevisiae* x *S. kudriavzevii,* 2 Far Eastern and 2 American *S. paradoxus* shown the GC cluster 7 in their *ORF1* sequences (Figure S3 and S11). Some GC clusters sequences were found inverted (Figure S3 and S11). GC cluster 7 of the two American *S. paradoxus* (120MX

and CBS5313) and three *S. cerevisiae*, two from Japan and one from USA (CBS435, Y9 and YPS606), contained identical GC cluster sequence (Figure S12). The confirmation of the American *S. paradoxus* mitochondrial background will shed light about the origin of this GC cluster, which simplest scenario is a transfer from the *S. cerevisiae* mitochondrial genome to *S. paradoxus ORF1*.

ORF1 GC clusters were classified according to Zamaroczy and Bernardi (de Zamaroczy and Bernardi 1986), except for GC cluster 2. GC cluster 1 and 4 are similar to a1 family, and GC cluster 3 and 5 were similar to a4 family. In the case of GC cluster 1, 2, 4, and 5 are on the opposite strand. As Séraphin *et al.* (1987) and Weiller *et al.* (1989) described, the GC clusters of the *ORF1* gene were flanked by TAG and AGGAG, or CTA and CTCCT when the cluster was inserted in the opposite strand (Figure S11). These conserved nucleotides were flanked by A+T rich sequences. Flanking sequences TAG and AG (CTA and CT) are conserved in most of the sequences with and without GC clusters. All GC clusters in *ORF1* belong to group M1 (Weiller *et al.* 1989). Conserved flanking regions might help to the transposition of GC clusters.

Differences in size were also due to the presence of AT repeats. Tandem repeat sequences for *COX2* and *ORF1* genes were detected and described using `Tandem Repeat Finder` software (Benson 1999). Twenty-one different A+T rich sequences that repeated at least twice were found in the *ORF1* alignment (Table S4). The length of A+T rich tandem repeats ranged from three nucleotides to twenty-five nucleotides. The most repeated sequence (AAT) was repeated ten times in haplotypes M1, M12, M22, M39, M40, and M50. The A+T rich tandem repeats were located near to GC clusters (Figure 6). In the *COX2* gene, we found three A+T rich sequences repeated twice (Table S4).

ORF1 detection of selection

The single likelihood ancestor counting (SLAC), fixed effects likelihood (FEL), and random effects likelihood (REL) methods (Pond and Frost 2005), implemented in the `HYPHY` web based version, `Datamonkey` (Delport *et al.* 2010), were used to detect the signatures of selection operating on the *ORF1* gene. NJ phylogenetic trees were reconstructed under the REV (GTR) substitution model. Two different approaches were performed to describe selection signatures. In the first approach, a complete *ORF1*

alignment, without GC Insertions and indels, partitioned by recombinant sections detected by GARD, was used. In a second study, the two LADGLIDADG and the NUMOD domains were analyzed independently.

Aminoacid positions were described as being under positive or purifying selection when significant values were generated by two of the three tested methods. Codon-specific selection pressure along the sequences (i.e. site specific dN-dS) was measured and *p*-values were estimated at each site. We analyzed 417 *ORF1* codons of the total 458. 61 codons, corresponding to 15% of the total, were found to be under purifying selection, where 43 of the 61 codons were found in LAGLIDADGs and NUMOD1 domains (Figure S9). A functional characterization might help to understand how important these aminoacids are for the activity of this homing endonuclease.

References

Almeida P, Gonçalves C, Teixeira S *et al.* 2014. A Gondwanan imprint on global diversity and domestication of wine and cider yeast *Saccharomyces uvarum*. Nat Commun. 5.

Altschul SF, Madden TL, Schaffer AA, Zhang J, Zhang Z, Miller W, Lipman DJ. 1997. Gapped BLAST and PSI-BLAST: a new generation of protein database search programs. Nucl Acids Res. 25:3389-3402.

Benson G. 1999. Tandem repeats finder: a program to analyze DNA sequences. Nucl Acids Res. 27:573-580.

Clark-Walker GD. 1991. Contrasting mutation rates in mitochondrial and nuclear genes of yeasts versus mammals. Curr Genet. 20:195-198.

Dalgaard JZ, Klar AJ, Moser MJ, Holley WR, Chatterjee A, Mian IS. 1997. Statistical modeling and analysis of the LAGLIDADG family of site- specific endonucleases and identification of an intein that encodes a site-specific endonuclease of the HNH family. Nucl Acids Res. 25:4626-4638.

de Zamaroczy M, Bernardi G. 1986. The GC clusters of the mitochondrial genome of yeast and their evolutionary origin. Gene. 41:1-22.

Delport W, Poon AFY, Frost SDW, Kosakovsky Pond SL. 2010. Datamonkey 2010: a suite of phylogenetic analysis tools for evolutionary biology. Bioinformatics. 26:2455-2457.

187 Gibbs MJ, Armstrong JS, Gibbs AJ. 2000. Sister-Scanning: a Monte Carlo procedure for
188 assessing signals in recombinant sequences. Bioinformatics. 16:573-582.
189 Guindon S, Gascuel O. 2003. A simple, fast, and accurate algorithm to estimate large
190 phylogenies by Maximum Likelihood. Syst Biol. 52:696-704.
191 Hittinger CT, Gonçalves P, Sampaio JP, Dover J, Johnston M, Rokas A. 2010.
192 Remarkably ancient balanced polymorphisms in a multi-locus gene network. Nature.
193 464:54-58.
194 James SA, Roberts IN, Collins MD. 1998. Phylogenetic heterogeneity of the genus
195 *Williopsis* as revealed by 18S rRNA gene sequences. Int J Syst Bacteriol. 48:591-596.
196 Leducq JB, Charron G, Samani P *et al.* 2014. Local climatic adaptation in a widespread
197 microorganism. Proc R Soc Lond B Biol Sci. 281:
198 Liti G, Carter DM, Moses AM *et al.* 2009. Population genomics of domestic and wild
199 yeasts. Nature. 458:337-341.
200 Livingstone C, Barton GJ. 1993. Protein sequence alignments: a strategy for the
201 hierarchical analysis of residue conservation. Comput Appl Biosci. 9:745-756.
202 Marchler-Bauer A, Anderson JB, Chitsaz F *et al.* 2009. CDD: specific functional
203 annotation with the Conserved Domain Database. Nucleic Acids Res. 37:D205-D210.
204 Martin D, Rybicki E. 2000. RDP: detection of recombination amongst aligned sequences.
205 Bioinformatics. 16:562-563.
206 Martin DP, Lemey P, Lott M, Moulton V, Posada D, Lefeuvre P. 2010. RDP3: a flexible
207 and fast computer program for analyzing recombination. Bioinformatics. 26:2462-2463.
208 Padidam M, Sawyer S, Fauquet CM. 1999. Possible emergence of new Geminiviruses
209 by frequent recombination. Virology. 265:218-225.
210 Peris D, Sylvester K, Libkind D, Gonçalves P, Sampaio JP, Alexander WG, Hittinger CT.
211 2014. Population structure and reticulate evolution of *Saccharomyces eubayanus* and its
212 lager-brewing hybrids. Mol Ecol. 23:2031-2045.
213 Pond SLK, Frost SDW. 2005. Datamonkey: rapid detection of selective pressure on
214 individual sites of codon alignments. Bioinformatics. 21:2531-2533.
215 Posada D. 2008. jModelTest: phylogenetic model averaging. Mol Biol Evol. 25:1253-
216 1256.

Salminen MO, Carr JK, Burke DS, McCutchan FE, Garcia-Martinez J. 1995. Identification of breakpoints in intergenotypic recombinants of HIV type 1 by bootscanning. AIDS Res Hum Retroviruses. 11:1423-1425.

Schmidt HA, Strimmer K, Vingron M, von Haeseler A. 2002. TREE-PUZZLE: maximum likelihood phylogenetic analysis using quartets and parallel computing. Bioinformatics. 18:502-504.

Séraphin B, Simon M, Faye G. 1987. The mitochondrial reading frame RF3 is a functional gene in *Saccharomyces uvarum*. J Biol Chem. 262:10146-10153.

Shimodaira H, Hasegawa M. 1999. Multiple comparisons of log-likelihoods with applications to phylogenetic inference. Mol Biol Evol. 16:1114-1116.

Smith JM. 1992. Analyzing the mosaic structure of genes. J Mol Evol. 34:126-129.

Strimmer K, Rambaut A. 2002. Inferring confidence sets of possibly misspecified gene trees. Proceedings Biological sciences / The Royal Society. 269:137-142.

Sun S, Evans BJ, Golding GB. 2011. "Patchy-Tachy" leads to false positives for recombination. Mol Biol Evol. 28:2549-2559.

Wang QM, Liu WQ, Liti G, Wang SA, Bai FY. 2012. Surprisingly diverged populations of *Saccharomyces cerevisiae* in natural environments remote from human activity. Mol Ecol. 21:5404-5417.

Waterhouse AM, Procter JB, Martin DMA, Clamp M, Barton GJ. 2009. Jalview Version 2--a multiple sequence alignment editor and analysis workbench. Bioinformatics. 25:1189-1191.

Weiller G, Schueller CME, Schweyen RJ. 1989. Putative target sites for mobile G+C rich clusters in yeast mitochondrial DNA: Single elements and tandem arrays. Mol Gen Genet. 218:272-283.

Wu B, Hao W. 2015. A dynamic mobile DNA family in the yeast mitochondrial genome. G3: Genes|Genomes|Genetics. 5:1273-1282.

Supplementary Tables and Figures

Table S1. Strain information.

Table S2. Primer pairs used in this study.

Table S3. Summary statistics for all *Saccharomyces* and each species using *COX2*.

Table S4. Distribution of AT tandem repeats.

Figure S1. *COX2* polymorphic sites.

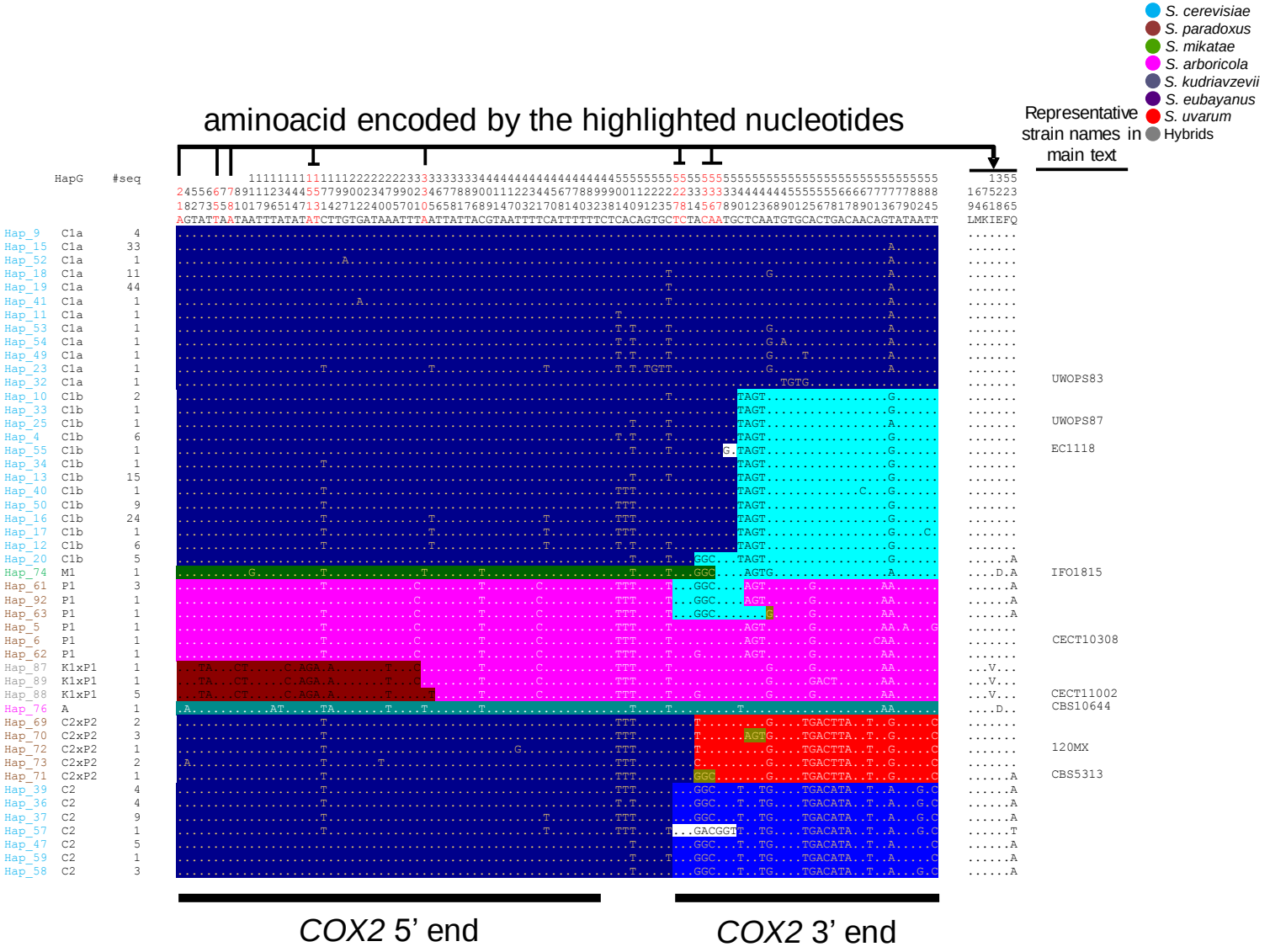

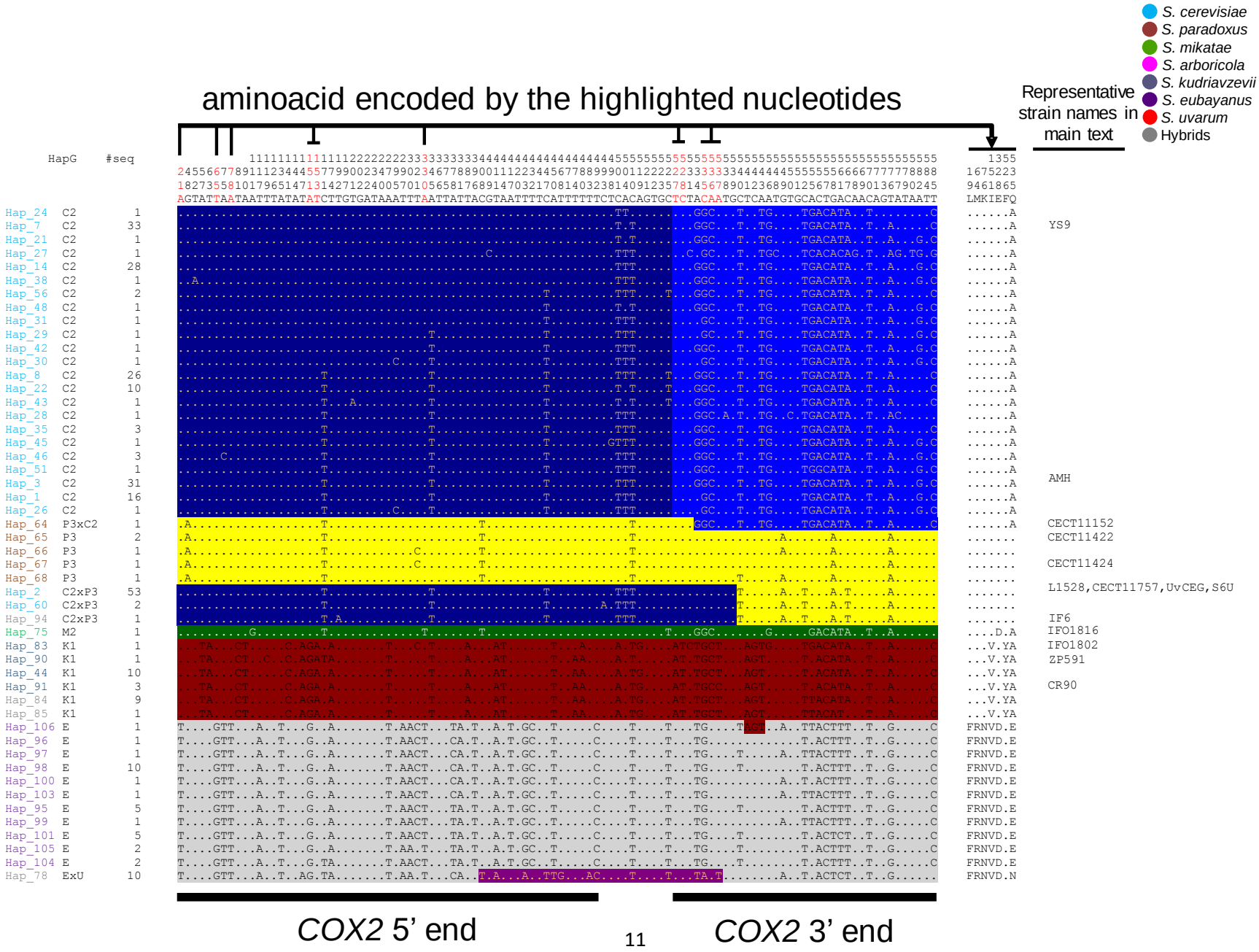
aminoacid encoded by the highlighted nucleotides
Representative strain names in main text
S. cerevisiae
S. paradoxus
S. mikatae
S. arboricola
S. kudriavzevii
S. eubayanus
S. uvarum
Hybrids
HapG
#seq
YS9
AMH
CECT11152
CECT11422
CECT11424
L1528,CECT11757,UvCEG,S6U
IF6
IFO1816
IFO1802
ZP591
CR90
COX2 5' end
COX2 3' end

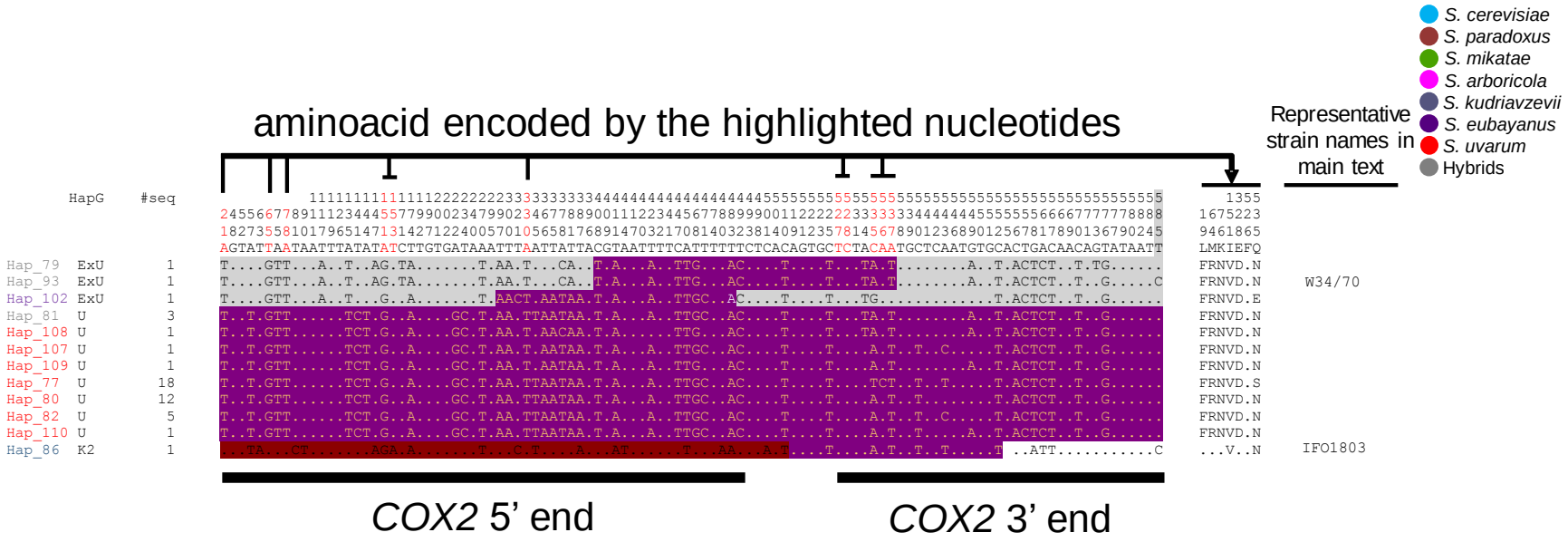

253

254 Variable *COX2* nucleotide positions, and discriminant aminoacids (in the right hand of the figure) encoded by highlighted
255 red nucleotides, are shown. Haplotype numbers are colored according to the species designation, according to Figure 2
256 and the legend. Numbers above polymorphic sites represent their position in the alignment. Black bars in the bottom
257 highlights the *COX2* regions used for reconstructing the phylogenetic networks in Figure S2. Haplogroup (HapG)
258 designation and the number of sequences (#seq) for each haplotype are shown in the left hand. The position in the alignment
259 of the first nucleotide for each codon, encoding the represented discriminant aminoacids, are shown above the aminoacid
260 sequence. Sequences were colored according to their similarity as inferred from Figure S2B. Strain names discussed in the
261 main text are represented in the right hand of their corresponding haplotype.

262

Figure S2. *COX2* Neighbor-Net phylogenetic network for each *COX2* segment.

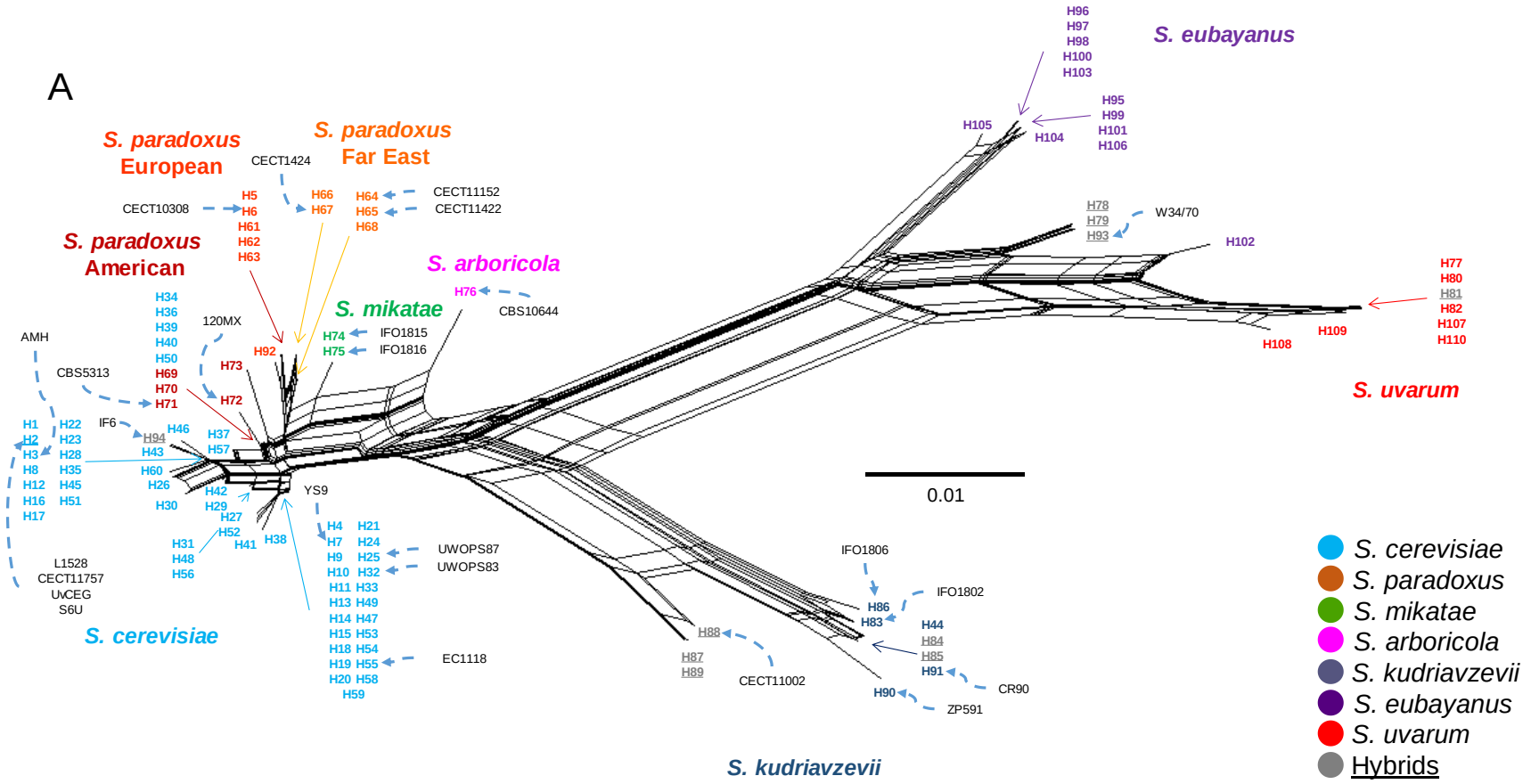

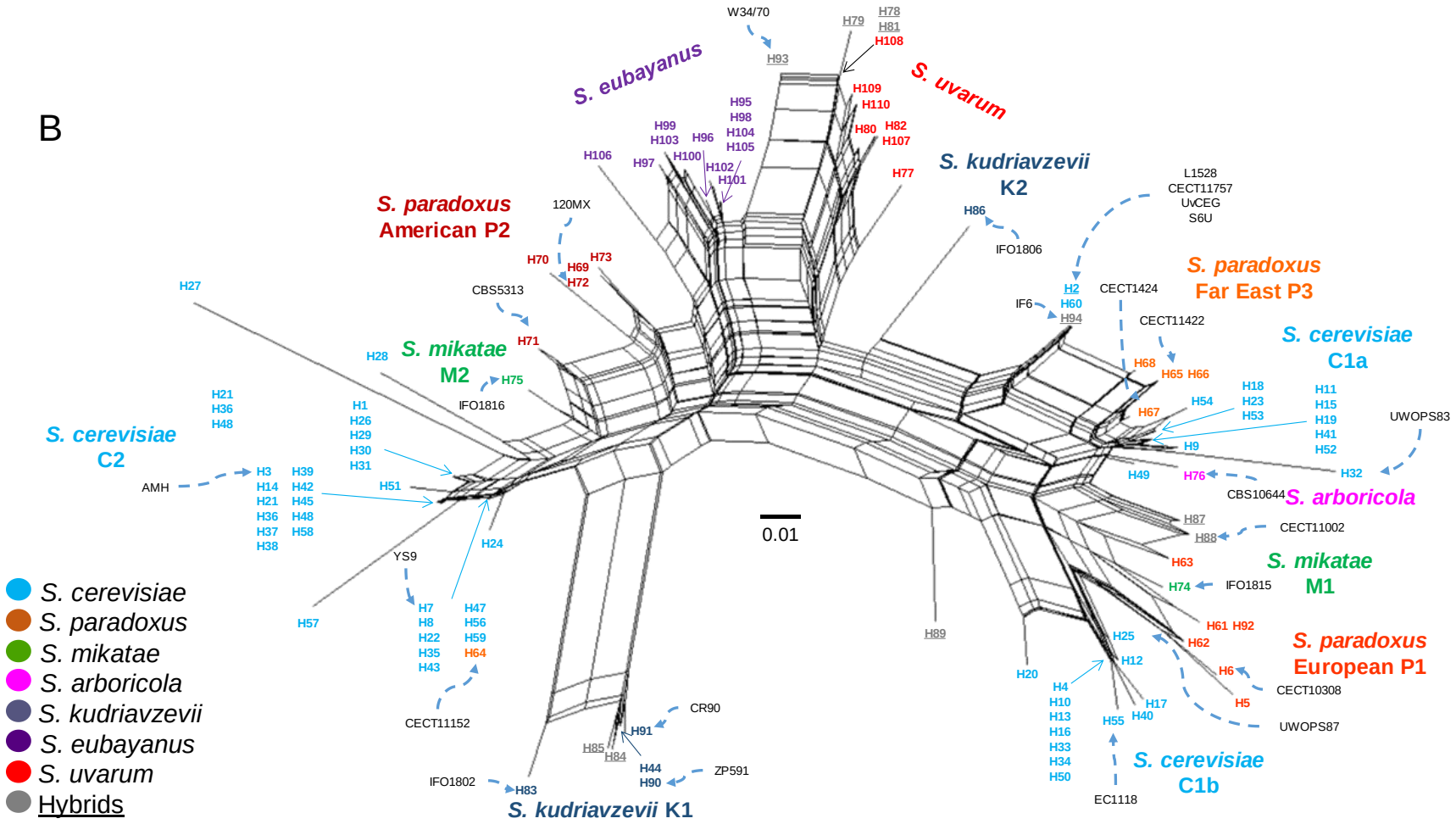

Reconstructed neighbor-net phylogenetic networks using the *COX2* 5' end, and 3' end segments are represented in A) and B), respectively. Haplotypes were colored according to each species designation. Haplotypes exclusively from hybrids are colored in grey. Scale is given in nucleotide substitution per site. Strain names discussed in the main text are represented and connected to their corresponding haplotype by a dashed blue arrow.

Figure S3. *ORF1* Neighbor-Joining phylogenetic tree.

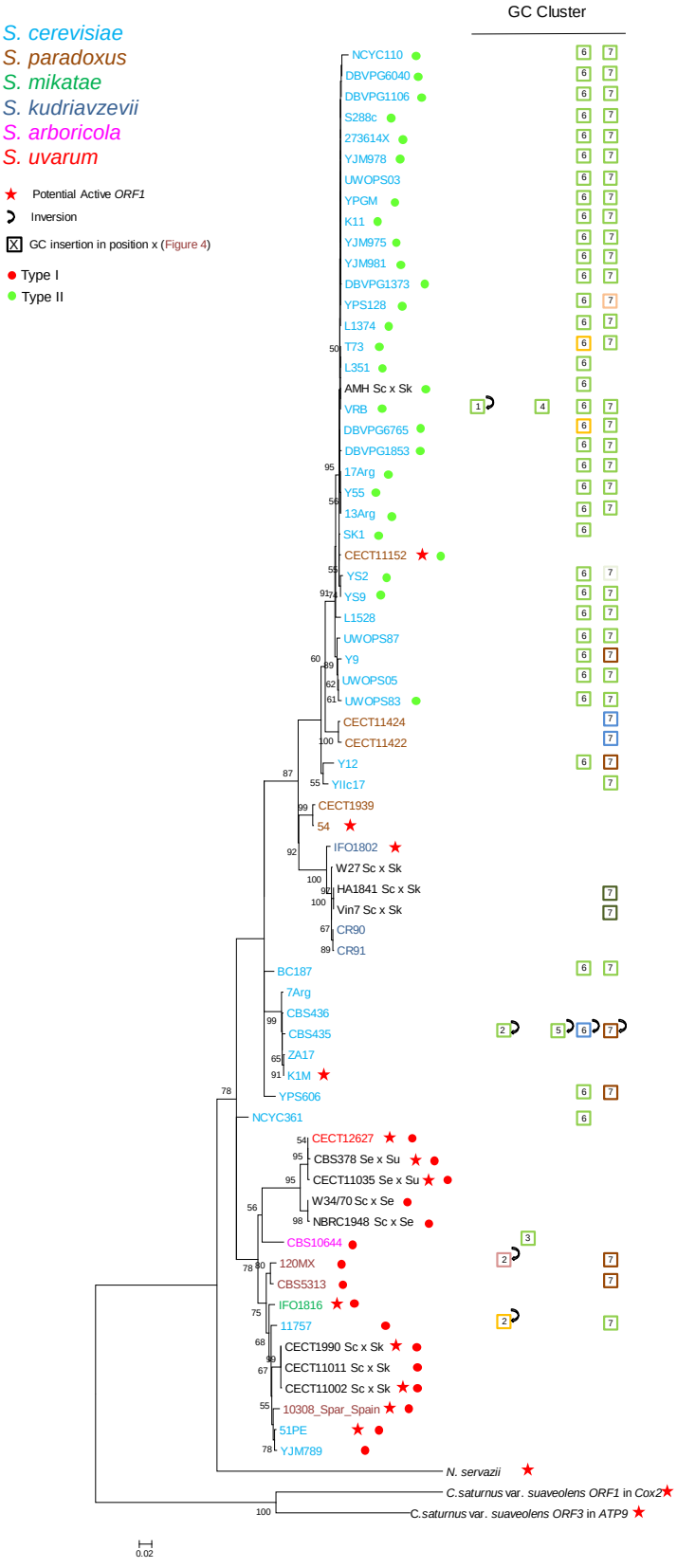

A NJ phylogenetic tree was reconstructed for the *ORF1* sequence alignment. Strains were colored according to the species designation. Bootstrap values above 50 are given for each branch. A red star represents a potential active *ORF1* based on the absence of GC clusters, which could disrupt the coding sequence, and premature stop codons. Type I and Type II *ORF1* sequences, detected as non-recombinant (represented by dots), were colored in red and green, respectively. GC clusters in the *ORF1* sequence were represented by squares and the number represents the position in the *ORF1* alignment (see Figure 6). An arrow indicates that a particular GC cluster was inverted to infer the GC cluster family. Square colors represent GC cluster similarity according to Figure S11, and the NJ trees from Figure S12.

Figure S4. *ORF1* aminoacid polymorphic sites.

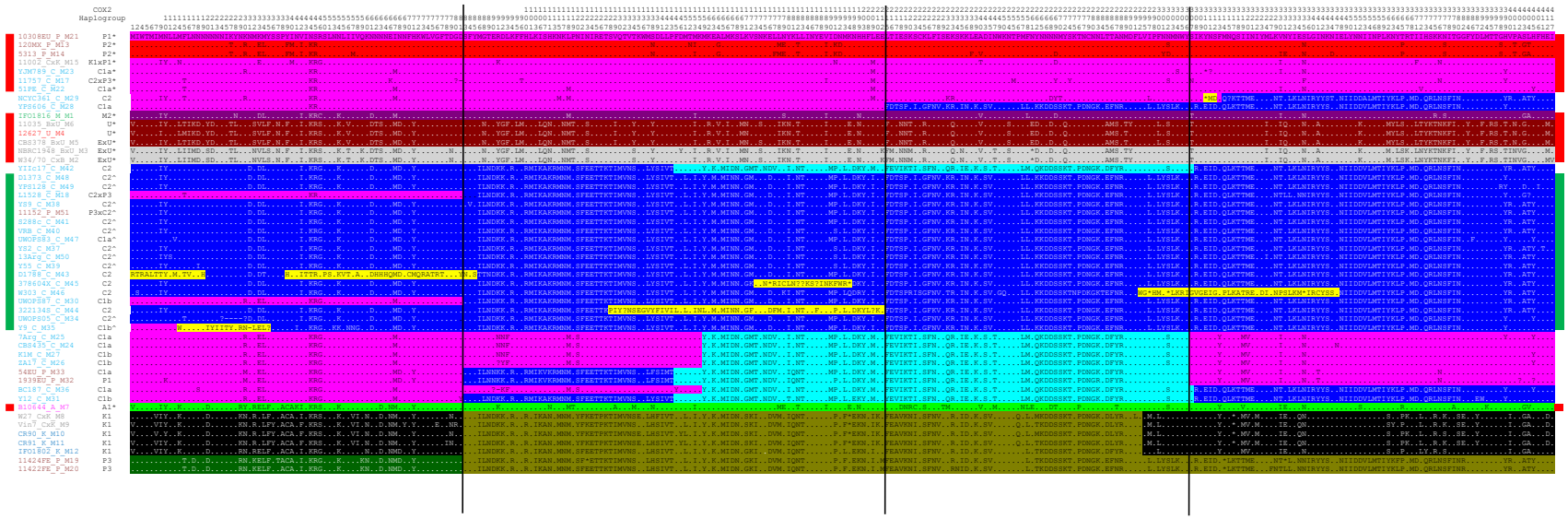

Variable *ORF1* aminoacid positions among haplotypes. Haplotype number are colored according to the species designation, as in Figure 2. Alignment aminoacid positions for each polymorphic site are also shown. The *COX2* Haplogroup designation is shown. Sequences were colored according to their similarity as inferred from Figure S5. Symbols * and ^ represent type I and type II *ORF1* sequences, respectively. Regions colored in yellow are sequences from unknown source. Lines indicate the sites corresponding to each alignment partition to reconstruct the *ORF1* phylogenetic networks by segments (Figure S5).

Figure S5. *ORF1* NN phylogenetic networks by segments.

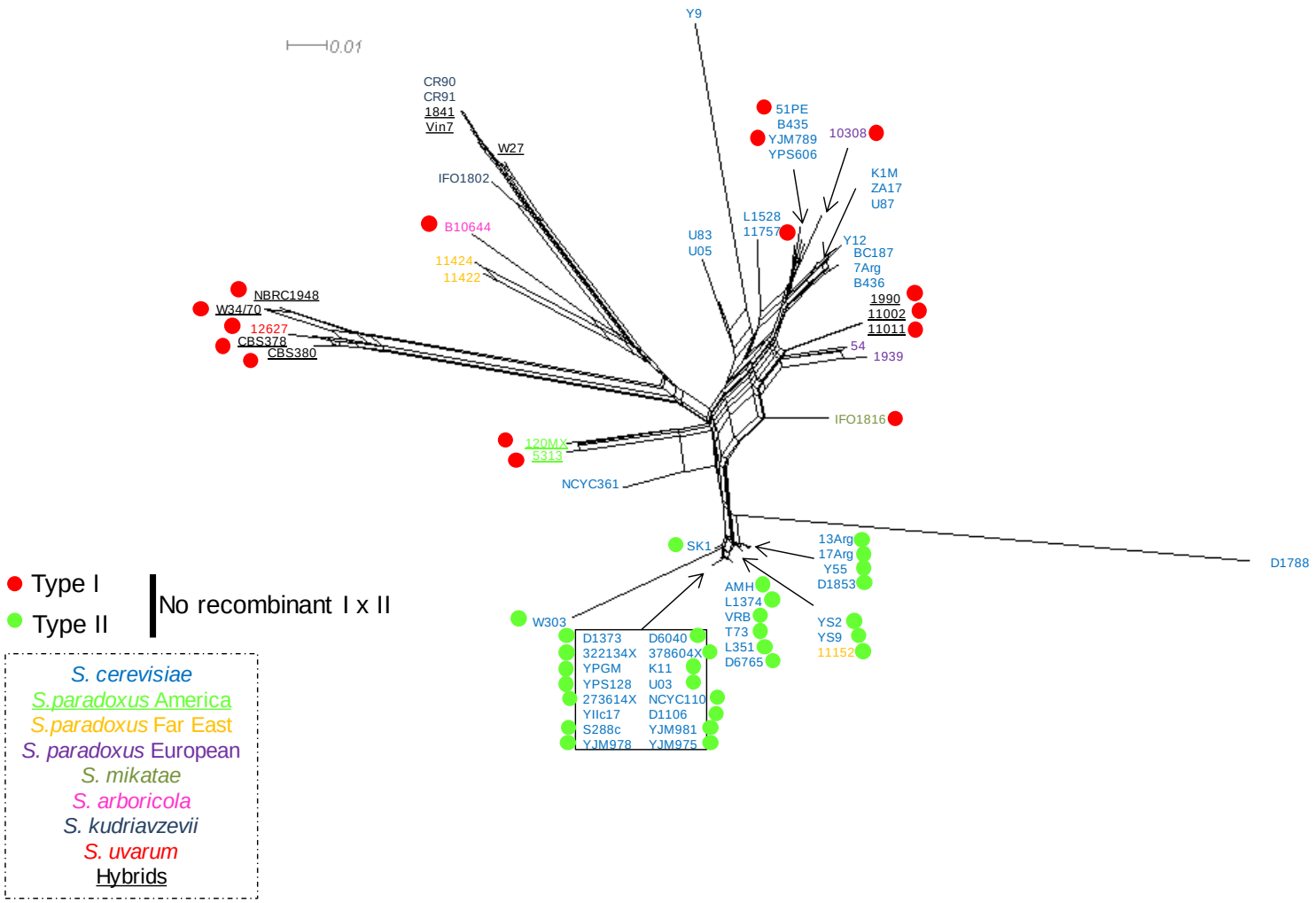

B

247-644

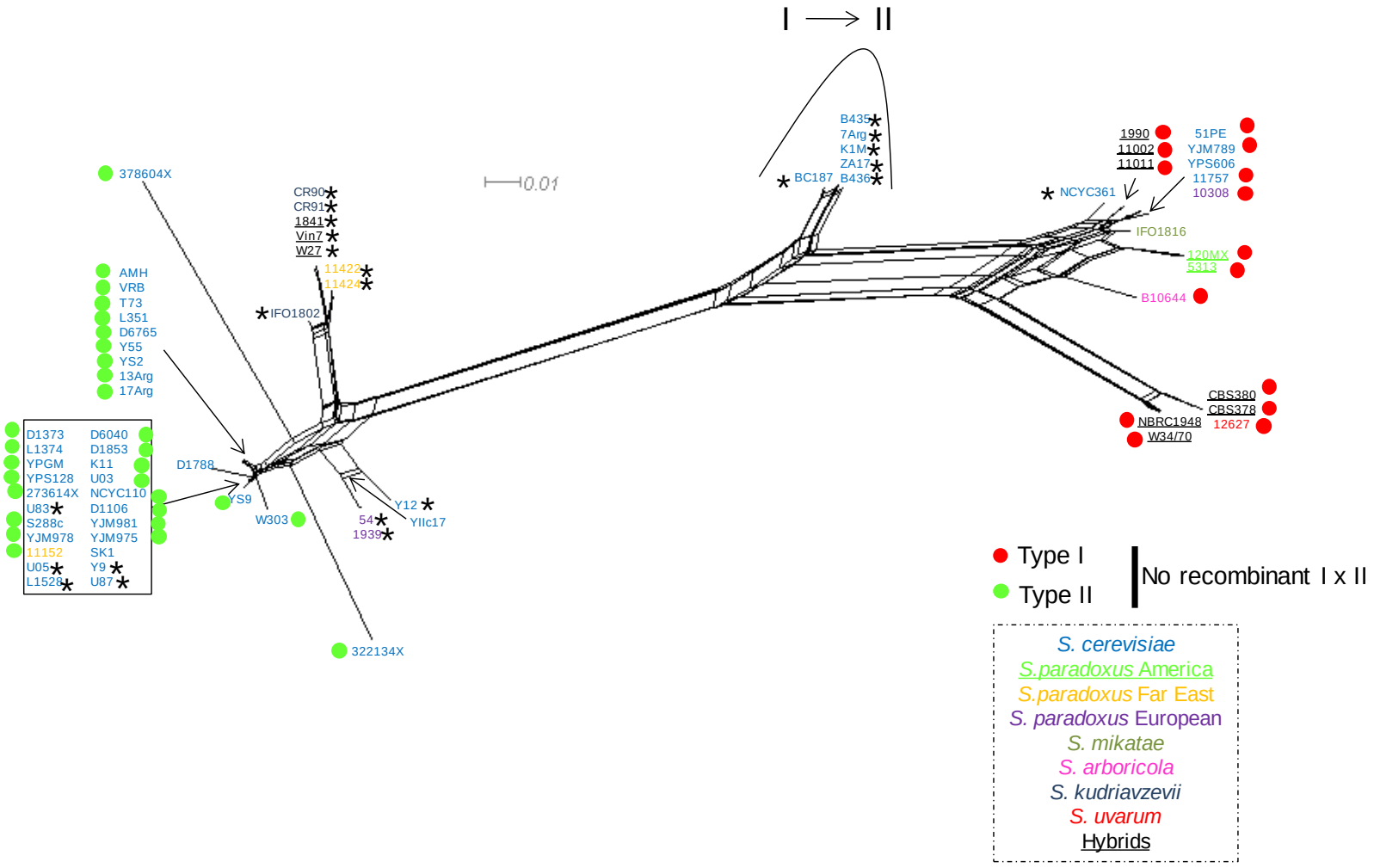
I → II
0.01
378604X
CR90
CR91
1841
Vin7
W27
11422
11424
IFO1802
AMH
VRB
T73
L351
D6765
Y55
YS2
13Arg
17Arg
D1373
L1374
YPGM
YPS128
273614X
U83
S288c
YJM978
11152
U05
L1528
D6040
D1853
K11
U03
NCYC110
D1106
YJM981
YJM975
SK1
Y9
U87
D1788
YS9
W303
54
1939
Y12
YIIc17
322134X
B435
7Arg
K1M
ZA17
B436
BC187
NCYC361
1990
11002
11011
51PE
YJM789
YPS606
11757
10308
IFO1816
120MX
5313
B10644
CBS380
CBS378
12627
NBRC1948
W34/70
Type I
Type II
No recombinant I x II
S. cerevisiae
S.paradoxus America
S.paradoxus Far East
S. paradoxus European
S. mikatae
S. arboricola
S. kudriavzevii
S. uvarum
Hybrids

294

C

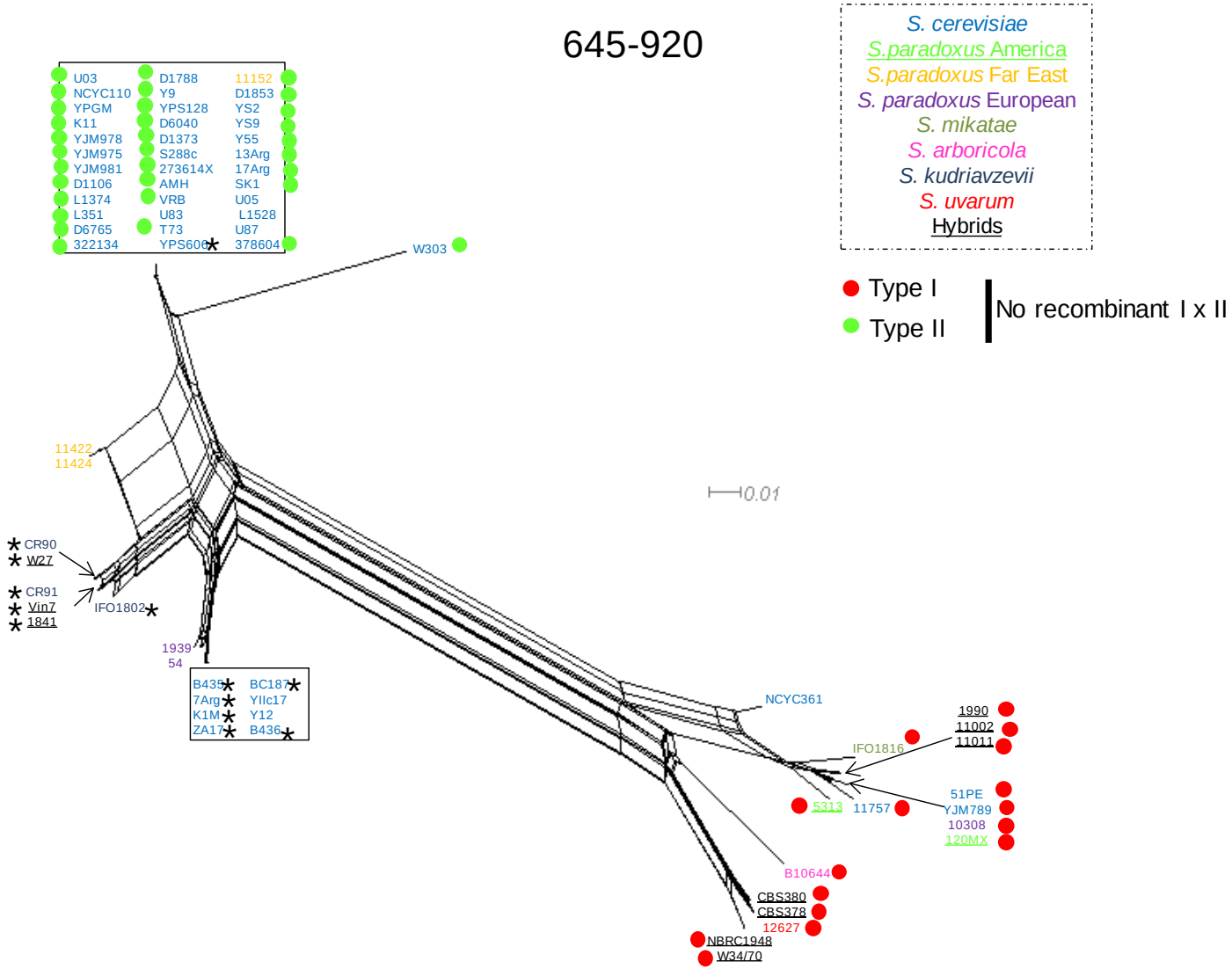
645-920
S. cerevisiae
S.paradoxus America
S.paradoxus Far East
S. paradoxus European
S. mikatae
S. arboricola
S. kudriavzevii
S. uvarum
Hybrids
Type I
Type II
No recombinant I x II
U03
NCYC110
YPGM
K11
YJM978
YJM975
YJM981
D1106
L1374
L351
D6765
322134
D1788
Y9
YPS128
D6040
D1373
S288c
273614X
AMH
VRB
U83
T73
YPS606
11152
D1853
YS2
YS9
Y55
13Arg
17Arg
SK1
U05
L1528
U87
378604
W303
11422
11424
0.01
CR90
W27
CR91
Vin7
1841
IFO1802
1939
54
B435
7Arg
K1M
ZA17
BC187
YIIc17
Y12
B436
NCYC361
1990
11002
11011
IFO1816
51PE
YJM789
10308
120MX
5313
11757
B10644
CBS380
CBS378
12627
NBRC1948
W34/70

295

296

297

D

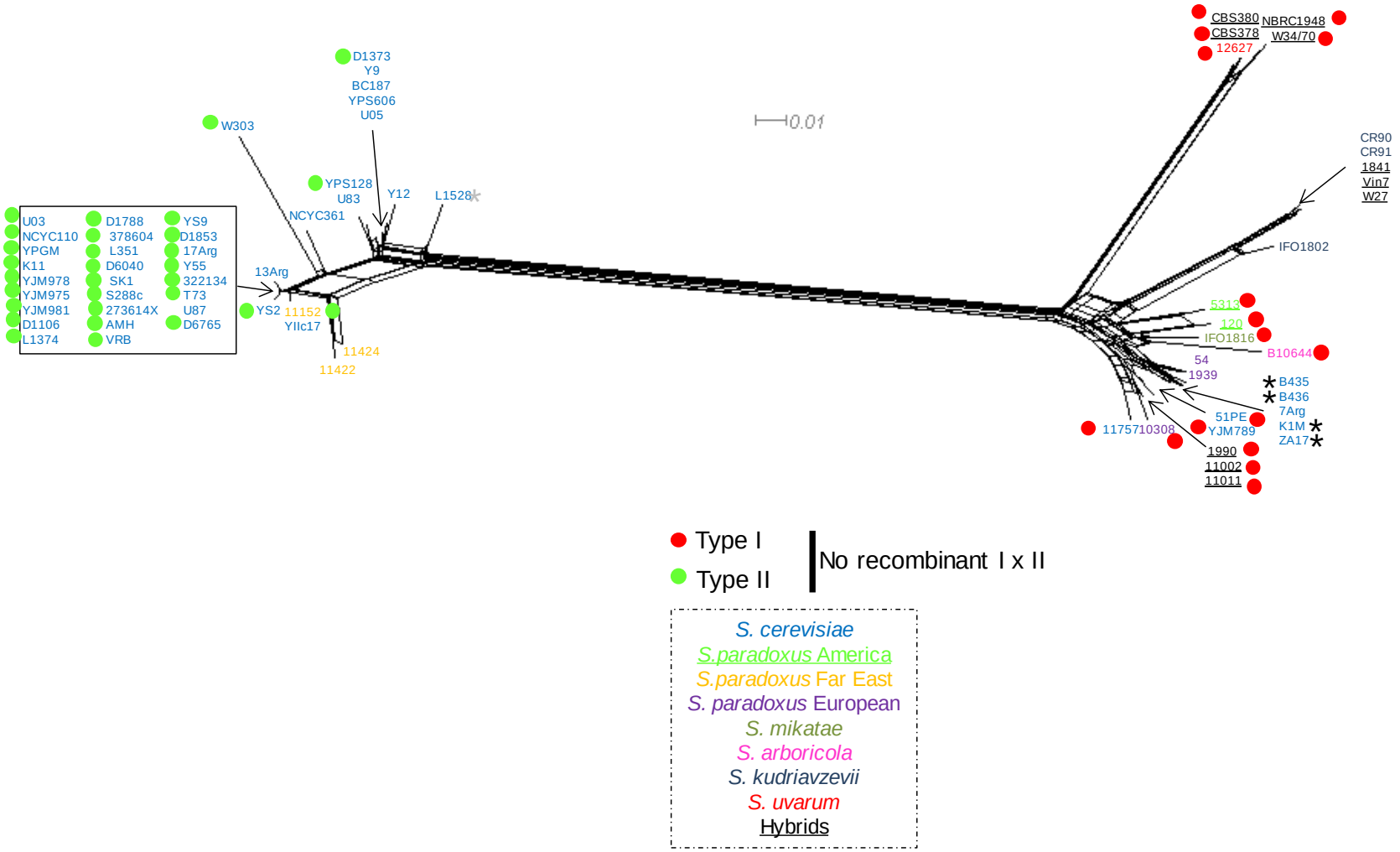
921-1251
0.01
U03
NCYC110
YPGM
K11
YJM978
YJM975
YJM981
D1106
L1374
D1788
378604
L351
D6040
SK1
S288c
273614X
AMH
VRB
YS9
D1853
17Arg
Y55
322134
T73
U87
D6765
W303
D1373
Y9
BC187
YPS606
U05
YPS128
U83
Y12
L1528
NCYC361
13Arg
YS2
11152
YIIc17
11424
11422
CBS380
NBRC1948
CBS378
W34/70
12627
CR90
CR91
1841
Vin7
W27
IFO1802
5313
120
IFO1816
B10644
54
1939
B435
B436
7Arg
K1M
ZA17
51PE
YJM789
1175710308
1990
11002
11011
Type I
Type II
No recombinant I x II
S. cerevisiae
S.paradoxus America
S.paradoxus Far East
S. paradoxus European
S. mikatae
S. arboricola
S. kudriavzevii
S. uvarum
Hybrids

298

NN phylogenetic networks. for each *ORF1* alignment partitions, inferred by GARD and RDP, are shown in A), B), C) and D). A) shows the NN phylogenetic network corresponding to the region from *COX2* 3' end (Figure S1) to the position 246 of the *ORF1* alignment. Nucleotide positions from *ORF1* alignment are shown in figures B-D. Scale bar are given in nucleotide substitution per site. Type I and Type II *ORF1* sequences, detected as non-recombinant, are represented by red and green circles, respectively. Sequences are colored to each species designation. In figure B) some *S. cerevisiae* sequences are grouped in a I -> II group, indicating that the region used for inferring that NN phylonetwork contains a recombination point for those particular strains driving to the ambiguous position. Asterisks highlight sequences which clustering changed from one *ORF1* type to another due to its recombinant character.

Figure S6. *COX3* NJ phylogenetic tree.

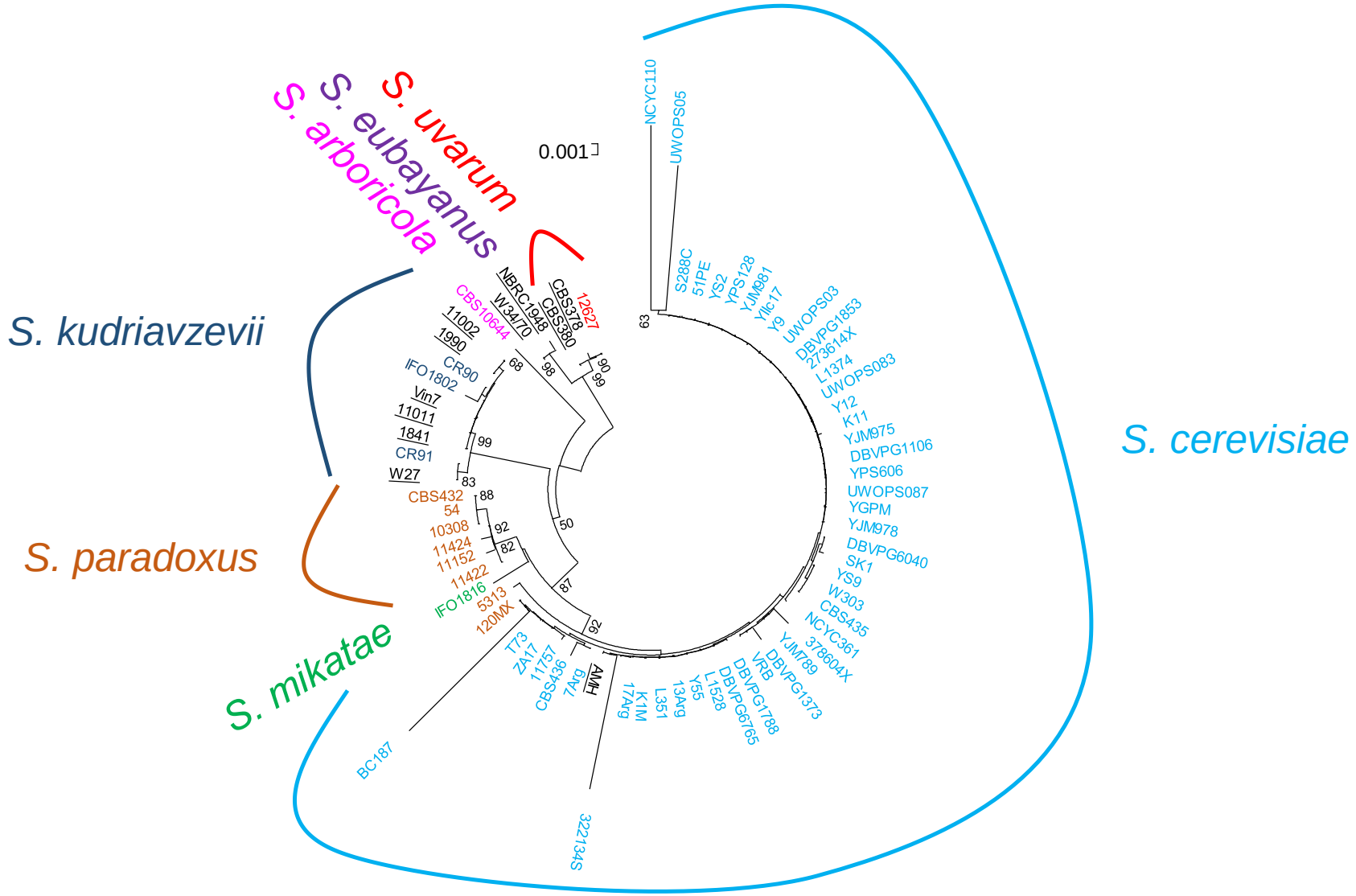

309 A *COX3* Neighbor-Joining phylogenetic tree is shown. Strains are colored according to the species designation. Bootstrap
310 values above 50 are given for each branch. Scale is given in nucleotide substitution per site.

Figure S7. *S. cerevisiae COX2* MJ networks.

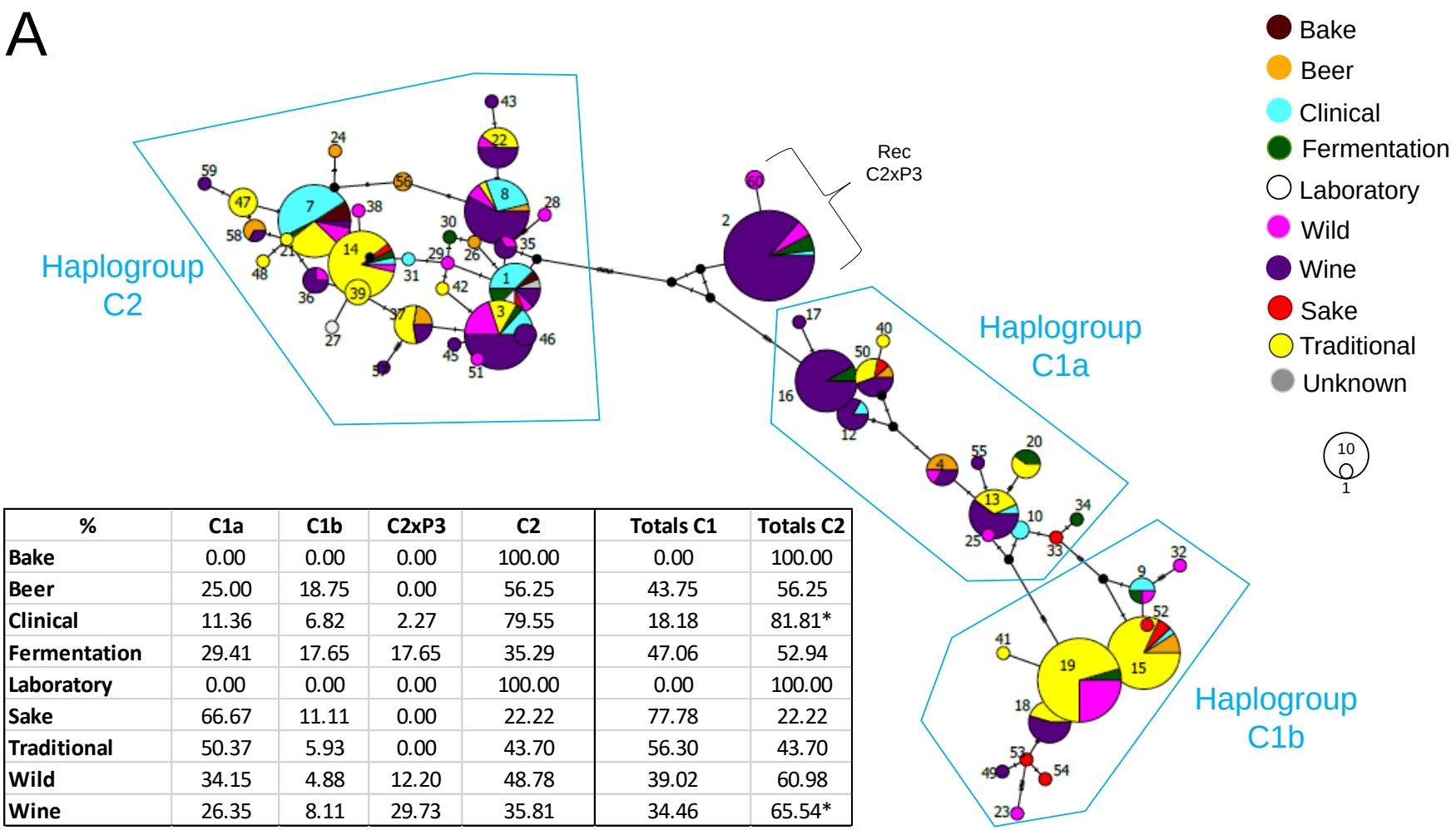

%	C1a	C1b	C2xP3	C2	Totals C1	Totals C2
Bake	0.00	0.00	0.00	100.00	0.00	100.00
Beer	25.00	18.75	0.00	56.25	43.75	56.25
Clinical	11.36	6.82	2.27	79.55	18.18	81.81*
Fermentation	29.41	17.65	17.65	35.29	47.06	52.94
Laboratory	0.00	0.00	0.00	100.00	0.00	100.00
Sake	66.67	11.11	0.00	22.22	77.78	22.22
Traditional	50.37	5.93	0.00	43.70	56.30	43.70
Wild	34.15	4.88	12.20	48.78	39.02	60.98
Wine	26.35	8.11	29.73	35.81	34.46	65.54*

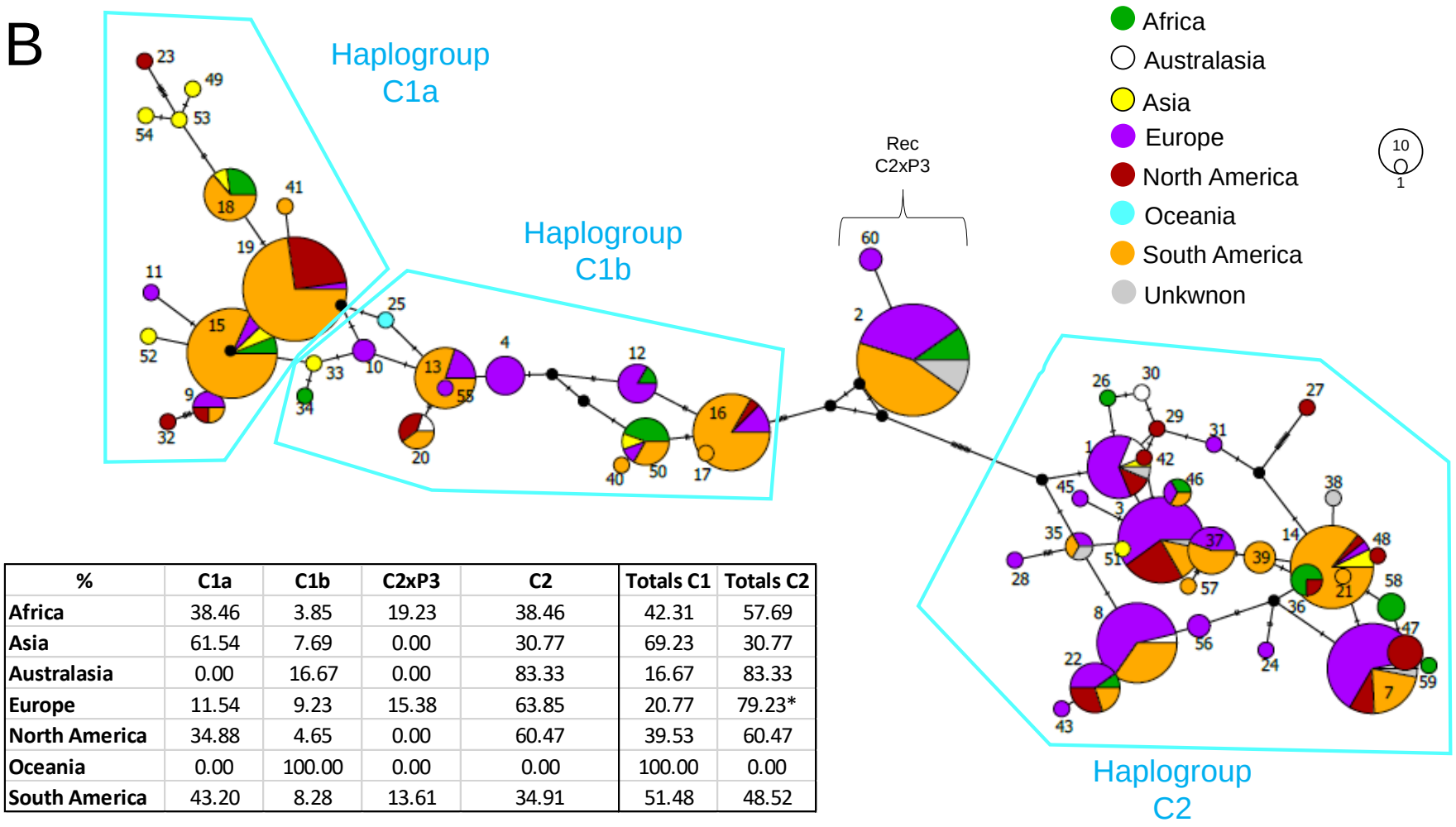

%	C1a	C1b	C2xP3	C2	Totals C1	Totals C2
Africa	38.46	3.85	19.23	38.46	42.31	57.69
Asia	61.54	7.69	0.00	30.77	69.23	30.77
Australasia	0.00	16.67	0.00	83.33	16.67	83.33
Europe	11.54	9.23	15.38	63.85	20.77	79.23*
North America	34.88	4.65	0.00	60.47	39.53	60.47
Oceania	0.00	100.00	0.00	0.00	100.00	0.00
South America	43.20	8.28	13.61	34.91	51.48	48.52

S. cerevisiae COX2 MJ networks were represented in A) and B) where haplotype pie charts were colored according to the isolation source and continent of isolation, respectively. Circle sizes represent the number of sequences in a haplotype and is scaled according to the legend. Number of mutations from one haplotype to another are indicated by lines in the edges

317 connecting the haplotypes. A table showing the strain percentage distribution in each haplogroup or recombinant group by
318 isolation source or continent is also displayed in A) and B), respectively.

Figure S8. A summary model of potential *COX2-ORF1* introgression in wild environments and during domestication.

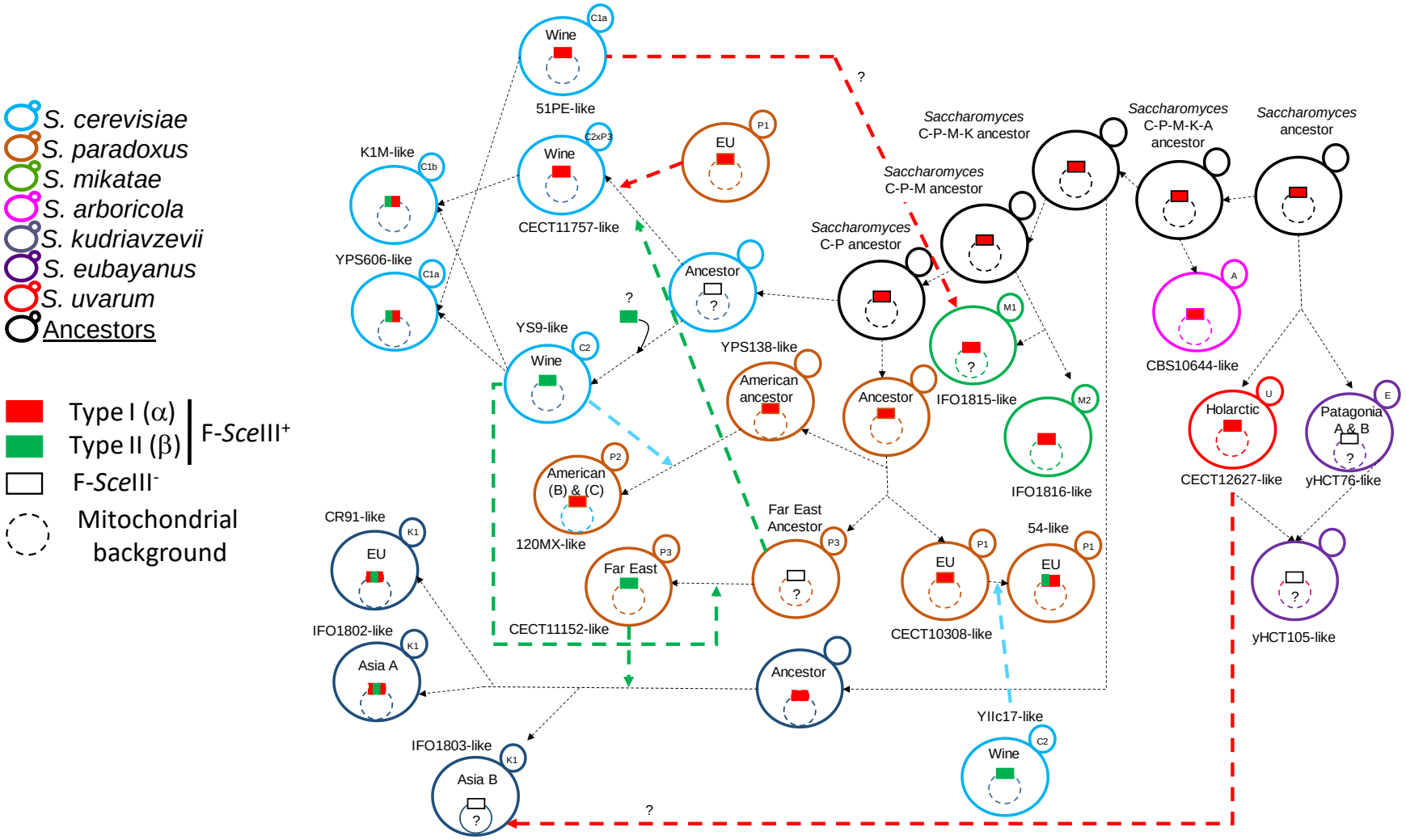

A starting model of potential introgressions in *Saccharomyces* is described. Black, light blue, orange, green, dark blue, pink, red and purple yeasts represent the yeast ancestors, *S. cerevisiae*, *S. paradoxus*, *S. mikatae, S. kudriavzevii, S. arboricola, S. uvarum* and *S. eubayanus* yeasts, respectively. Small circles inside yeasts represent the mtDNA, which is colored according to the species designation. A *S. paradoxus* yeast with a blue small circle indicates a potential inheritance of mtDNA from *S. cerevisiae*. Red, green or red/green boxes represent type I, type II or recombinant *ORF1* sequences, respectively. A question tag indicates dubious scenario, unknown *ORF1* or unknown mtDNA sequence due to the absence of *COX3* sequence to support the mtDNA inheritance.

Figure S9. Weblogo representation of LAGLIDADG and NUMOD domains.

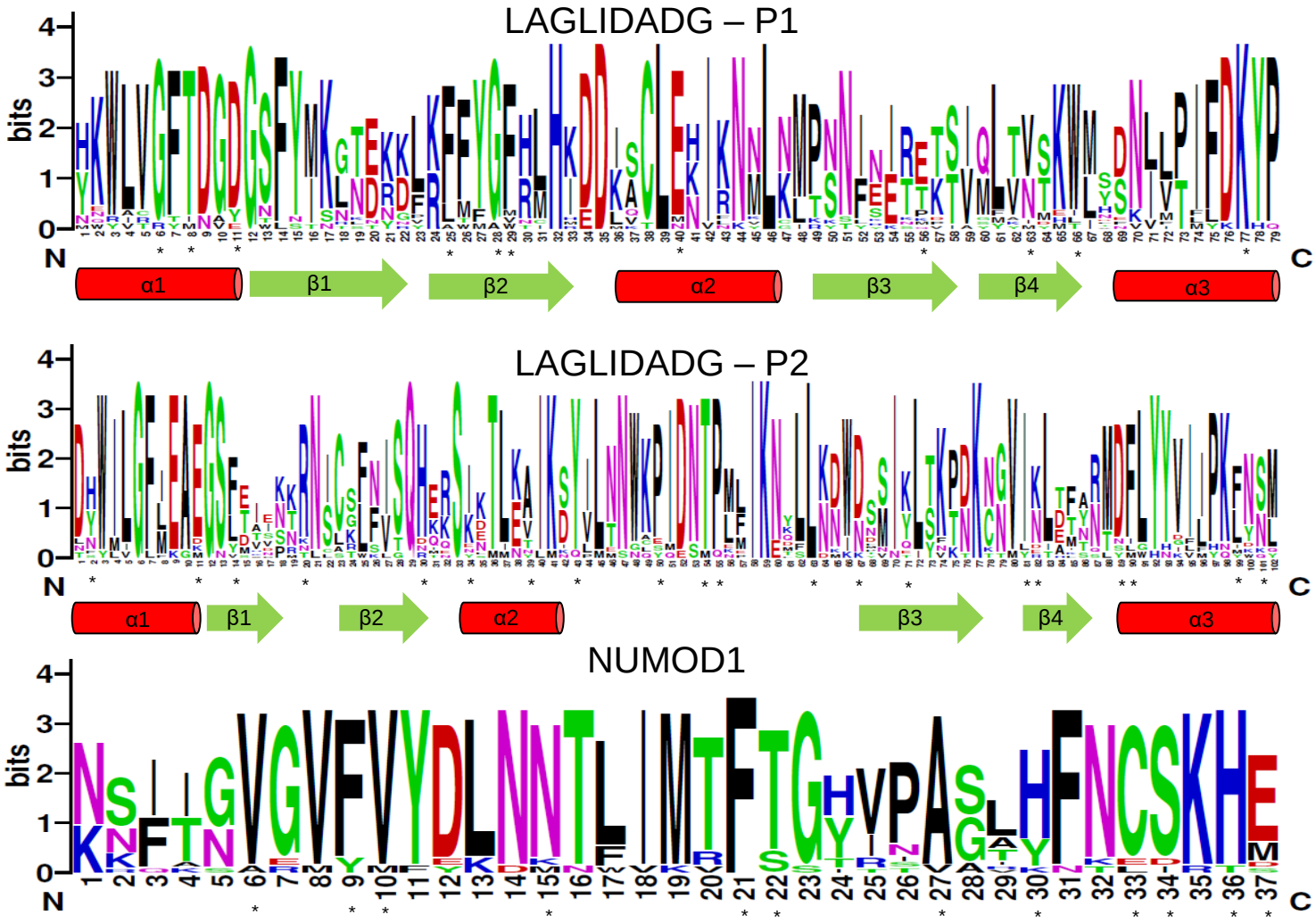

Weblogo (http://weblogo.berkeley.edu/) of the three homing endonuclease domains for *Saccharomyces ORF1* genes plus *SasefMp08* from *Kazchastania servazii*, and *ORF1* and ORF3 from *Cyberlindnera* (*Williopsis*) *saturnus* var. *suaveolens* are

represented. Cylinders and arrows represent α-helix and β-sheet, as previously described (Dalgaard *et al.* 1997). Asterisk symbol indicates the codons for those aminoacids under purifying selection detected by `DataMonkey`.

Figure S10. *COX2* and *ORF1* aminoacid alignment (Supplementary File Figure S10).

The complete *COX2* and *ORF1* aminoacid alignments are shown. Protein secondary structure and domains are indicated for *ORF1.* Jalview also display the alignment quality (based on BLOSUM 62), physicochemical conservation calculated according to Livingstone and Barton (Livingstone and Barton GJ 1993), and consensus sequence.

Figure S11. GC clusters from M1 family insertion regions.

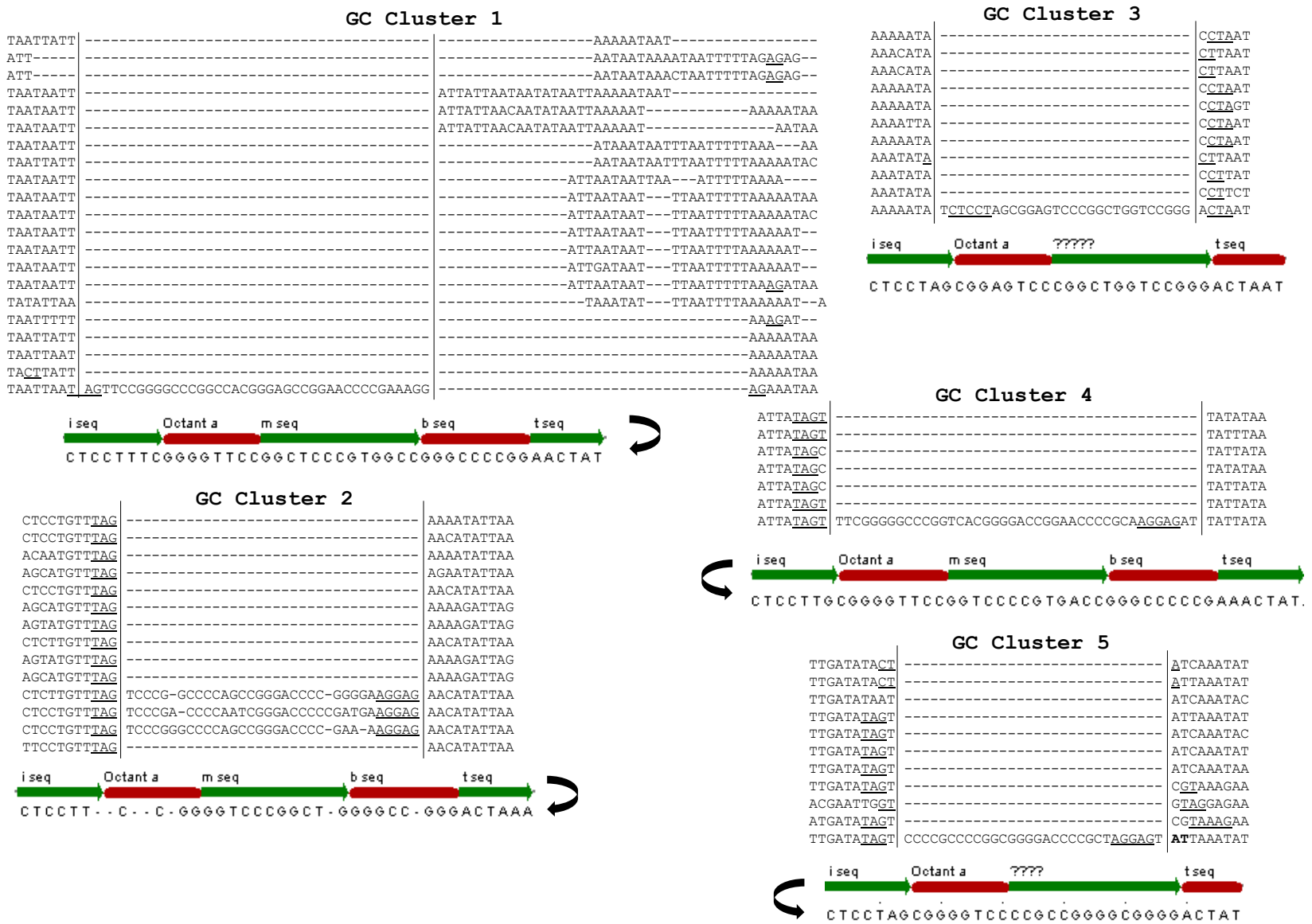

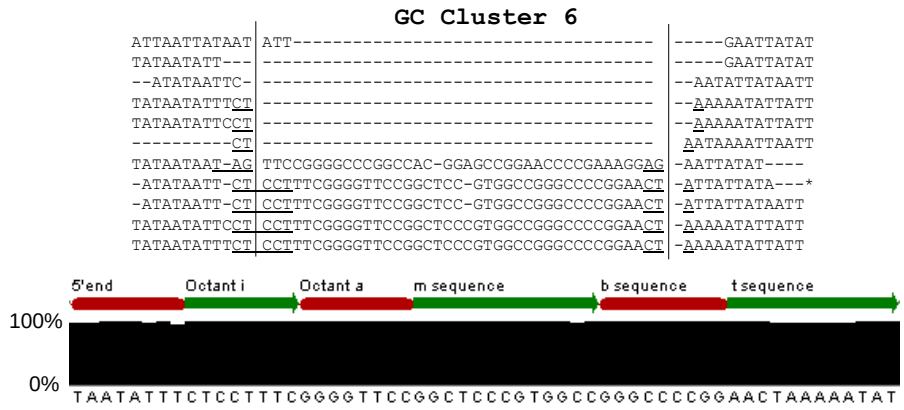

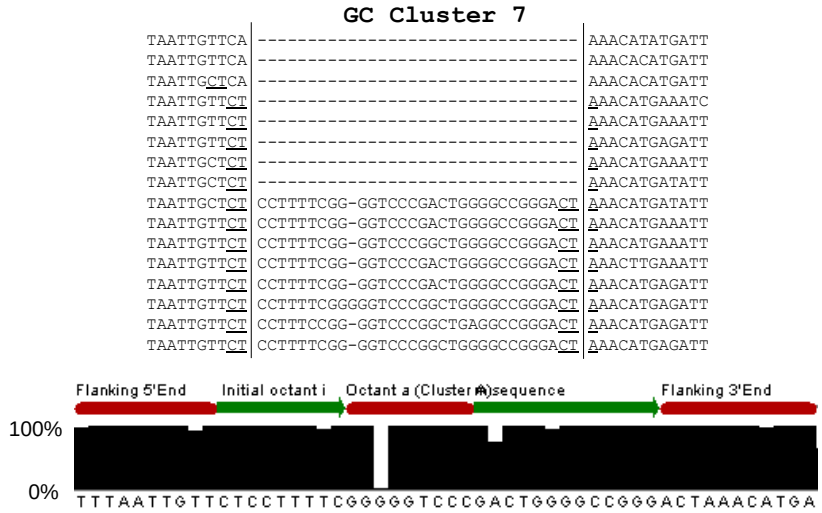

The flanking regions where the seven GC clusters were found are shown. In the case of GC cluster 6 and 7 a consensus sequence is shown and bars show the percentage of sequences showing a particular nucleotide substitution. An arrow indicates that the GC cluster sequence was inverted to annotate its structure. Question marks indicate an unknown GC cluster structure.

Figure S12. GC cluster 6 and 7 Neighbor-Joining phylogenetic trees.

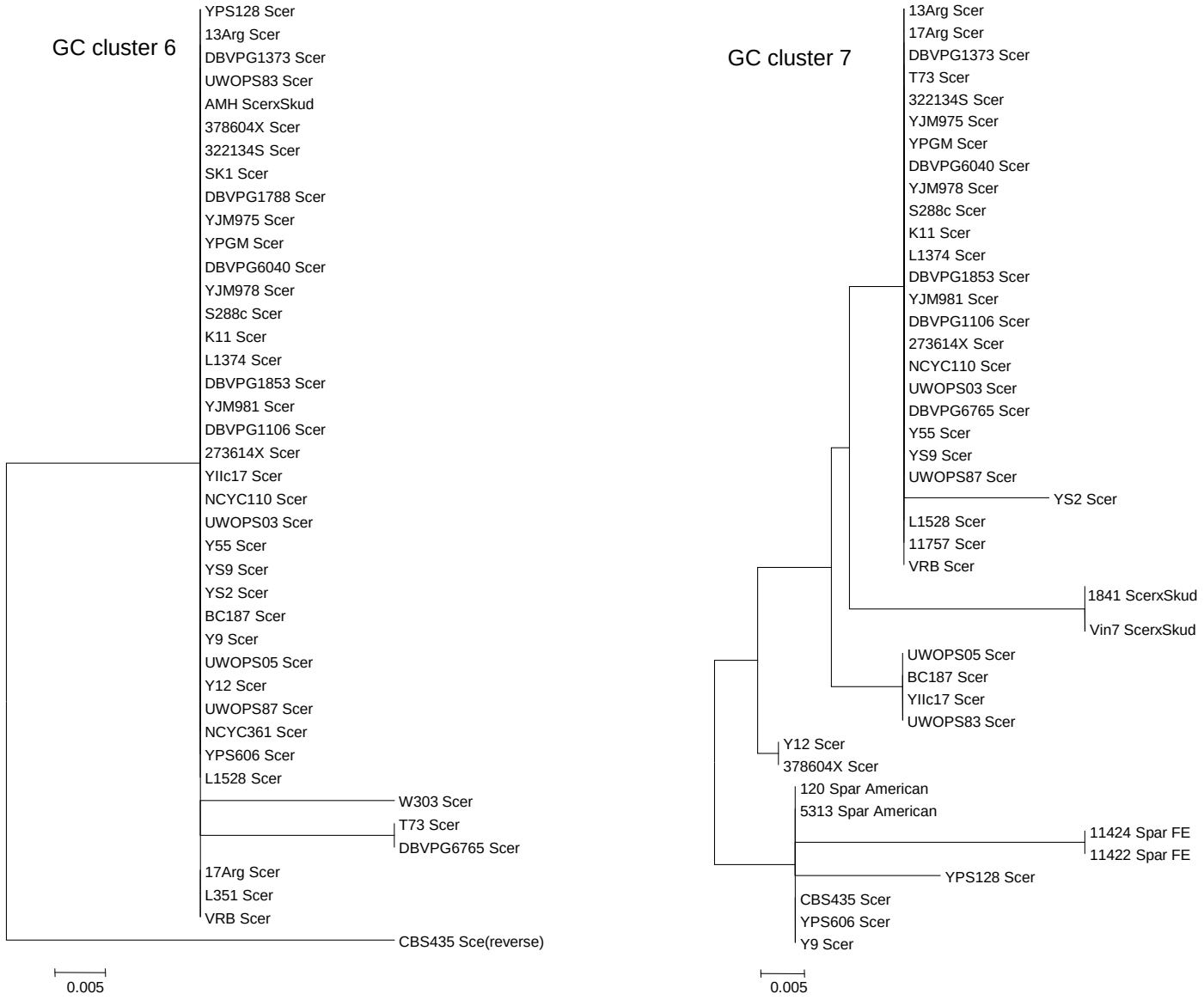

To classify the GC cluster according to sequence similarity we reconstructed the NJ phylogenetic tree of GC cluster 6 and 7. This classification is shown by numbers in Figure S3. Scale bars represent number of substitutions per site.